

# MHD Free Convective Flow through Porous Medium under the Effects of Radiation and Chemical reaction

D Chenna Kesavaiah<sup>1</sup>, R S Jahagirdar<sup>2</sup>

<sup>1</sup>Department of Humanities & Science, K G Reddy College of Engineering & Technology, Chilkur, Moinabad, R R Dist, TS - 501504, India

<sup>2</sup>Department of Mechanical Engineering, K G Reddy College of Engineering & Technology, Chilkur, Moinabad, R R Dist, TS - 501504, India

**Abstract**-This paper focused on magnetohydrodynamic free convection mass transfer and chemically reacting fluid flow interruption at unvarying heat flux and enclosed firmly through porous medium in a viscous fluid concentrated past a moving plate were considered. The governing partial differential equations are solved analytically by using perturbation technique. Solutions for the velocity profiles, temperature profiles, concentration profiles, skin friction, rate of heat and mass transfer are noticeable graphically for different values of physical parameters connected in the present problem. The results of our study agree well with the previous solution.

**Keywords:** Natural Convection, Chemically reacting fluid, Porous Medium

## I. INTRODUCTION

Consider in detail and subject to an analysis in order to discover essential features of natural convection flow accompanying mass transfer through the effect of chemical reaction have been concerned applications in large number of areas such as science, engineering and manufacturing process. This remarkable development plays a great significance activity in the chemical industry, wire drawing, continuous casting and fibre drawing, petroleum industry, power industries, chemical process industries, cooling of nuclear reactors, hot extrusion, wire drawing and continuous casting processes, hot rolling, just quiescent ambient air. In most cases, the moving material is hotter than the surroundings, and the heat transfer to the ambient occurs at the surface of the moving material. In view of the above the effects of chemical reaction and variable viscosity on hydromagnetic mixed convection heat and mass transfer of Hiemenz flow through porous media has been studied in the presence of radiation and magnetic field studied by Seddeek et.al [11]. Mohamed Abd El-Aziz et.al [13] has been investigated an unsteady magnetohydrodynamic free convection flow past a moving plate maintained at constant heat flux and embedded in a viscous fluid saturated porous medium of simultaneous effects of thermal and concentration diffusions. Ch Kesavaiah et.al [18] analyzed analytical for heat and mass transfer by laminar flow of a Newtonian, viscous, electrically conducting and heat generation/absorbing fluid on a continuously vertical permeable surface in the presence of a radiation, a first order homogeneous chemical reaction and mass flux. Chenna Kesavaiah et.al [21] examined the influence of chemical reaction on MHD mixed convection heat and mass transfer for a viscous fluid past an infinite vertical plate embedded in a porous medium with radiation and heat generation. Ch Kesavaiah et. al. [22] have studied the effect of the steady two dimensional free convection heat and mass transfer flow electrically conducting and chemically reacting fluid through a porous medium bounded by a vertical infinite surface with constant suction velocity and constant heat flux in the presence of a uniform magnetic field.

Convection toward the inside of porous media has acquire significant attention in recent years because of its prominent status in engineering applications such as geothermal systems, fibrous insulation and catalytic reactors to geological strata, gas or liquid matrix heat exchangers, thermal isolated (insulations), nuclear waste disposal, oil attributes, geothermal reservoirs, storage of heat generating tangible substances and store of nuclear waste materials. Convection in porous media can also be applied to underground coal gasification, ground water hydrology, iron blast furnaces, wall cooled catalytic reactors, solar power collectors, energy efficient drying processes, cooling of nuclear fuel in shipping flasks, cooling of electronic equipment and natural convection in earth's crust and non –Darcy effects on momentum, energy, and mass transport in porous media have been studied in depth for various geometrical configurations and boundary conditions. With these applications several studies are brought together in a broad scope examine of convective heat transfer process through porous media by Nield and Bejan [5], Kim [8], Chamkha [1, 2], Hayat and Abbas [10].

The study of convective flow with heat and mass transfer under the influence of chemical reaction has practical application is many areas of science and engineering. This phenomenon plays an important role in the chemical industry, petroleum industry, cooling of nuclear reactors, and packed bed catalytic reactors, so that it has received a considerable amount of attention in recent years. In view of the above some of the authors related research work studied by Ch Kesavaiah [12] Effects of radiation and free convection currents on unsteady Couette flow between two vertical parallel plates with constant heat flux and heat source through porous medium, Karunakar Reddy et.al. [13] MHD heat and mass transfer flow of a viscoelastic fluid past an impulsively started infinite vertical plate with chemical reaction, Ch Kesavaiah et.al. [14] Radiation and mass transfer effects on moving vertical plate with variable temperature and viscous Dissipation, Chenna Kesavaiah et.al. [15] Radiation and Thermo - Diffusion effects on mixed convective heat and mass transfer flow of a viscous dissipated fluid over a vertical surface in the presence of chemical reaction with heat source, Ch Kesavaiah et.al. [16] Radiation absorption, chemical reaction and magnetic field effects on the free convection and mass transfer flow through porous medium with constant suction and constant heat flux.

This paper focused on an unsteady magnetohydrodynamic free convection mass transfer and chemically reacting flow continued at unvarying heat flux and enclosed firmly through porous medium in a viscous fluid gathered together past a moving plate were considered. The governing partial differential equations are solved analytically by using perturbation method.

## II. FORMULATION OF THE PROBLEM

We focused on an unsteady one - dimensional chemically reacting and mass transfer, radiating flow of a viscous, electrically conducting an incompressible fluid an infinite vertical plate through embedded in a porous medium with constant heat flux at axis  $y' = 0$  and  $x'$  - axis is fixed along the plate in the lower to higher direction,  $y'$  - axis is measured normal to the plate in the outward direction. A uniform magnetic field  $B_0$  performance in the transverse point to the flow.

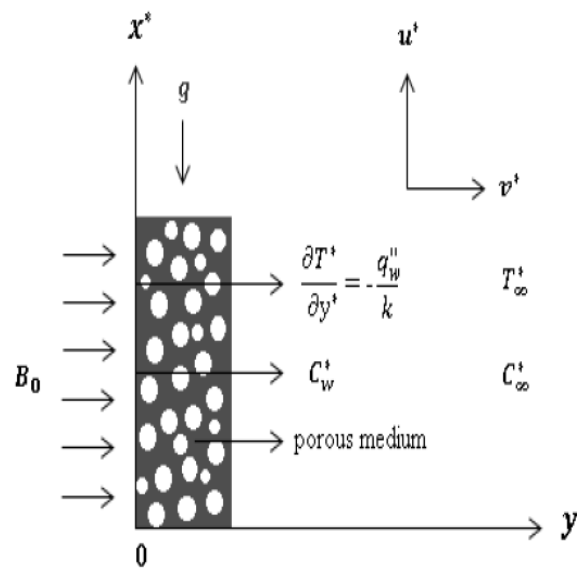


Figure (1): Physical coordinate system

The magnetic Reynolds number and transversely applied magnetic field are adopted in order to decrease to be below average so that the Hall Effect and induced magnetic field are negligible. The thermal buoyancy and Soret effects are also taken into account. The plate is infinite in length, so all the fields are adequate to enhance the appearance of functions of space coordinate  $y^*$  and time  $t'$ . At the beginning, the plate and the fluid are at uniform temperature  $T_\infty'$  and concentration  $C_\infty'$ . Subsequently, at time  $t' > 0$ , the plate begins to move in its own plane and accelerates against the gravitational field with uniform acceleration  $f(t')$  in  $x'$ -direction. At the same instant, heat is necessary from the surface of the plate to the fluid, which is continued all the way through the fluid flow at the uniform rate  $\frac{q_w''}{k}$  and concentration level, is increased to  $C_w''$  as shown in figure (1).

Insufficiently the above proposal and bring into the state of the Boussinesq approximation, the governing partial differential equations of the momentum, energy and concentration equations are governed by:

$$\frac{\partial u'}{\partial t'} = \nu \frac{\partial^2 u'}{\partial y'^2} - \frac{\sigma B_0^2}{\rho} u' - \frac{\nu}{K'} u' + g \beta (T' - T_\infty') + g \beta' (C' - C_\infty') \tag{1}$$

$$\rho c_p \frac{\partial T'}{\partial t'} = \kappa \frac{\partial^2 T'}{\partial y'^2} - \frac{\partial q_r'}{\partial y'} - Q_0 (T' - T_\infty') \tag{2}$$

$$\frac{\partial C'}{\partial t'} = \kappa \frac{\partial^2 C'}{\partial y'^2} - Kr' (C' - C_\infty') \tag{3}$$

The initial and boundary conditions for equations are

$$u' = 0, \quad T' = T_\infty', \quad C' = C_\infty' \quad \forall \quad y' \geq 0, \quad t' \leq 0$$

$$u' = f(t'), \quad \frac{\partial T'}{\partial y'} = -\frac{q_w''}{k}, \quad C' = C_\infty' \quad \text{at} \quad y' = 0, \quad t' > 0 \tag{4}$$

$$u' \rightarrow 0, \quad T' \rightarrow T_\infty', \quad C' \rightarrow C_\infty' \quad \text{as} \quad y' \rightarrow \infty$$

in which  $f(t')$  is the uniform acceleration of the plate,  $x'$  and  $y'$  are the distances along and perpendicular to the plate,  $u^*$  is the fluid velocity in the  $x'$ -direction,  $T'$  is the temperature of the fluid,  $t'$  is the dimensional time,  $T'_\infty$  is the free stream temperature,  $C'$  is the concentration,  $C'_w$  is the surface concentration,  $C'_\infty$  is the free stream concentration,  $q'_r$  is the radiative heat flux in  $x'$ -direction,  $\kappa$  is the thermal conductivity,  $q_w''$  is the constant heat flux per unit area at the plate,  $Q_0$  is the dimensional heat absorption coefficient,  $\beta'$  is the volumetric coefficient of expansion for concentration,  $\beta$  is the volumetric coefficient of thermal expansion,  $\mu$  is the fluid viscosity,  $\rho$  is the fluid density,  $\nu$  is the kinematic viscosity,  $\sigma$  is the electrical conductivity of the fluid,  $c_p$  is the specific heat capacity,  $K'$  is the permeability of the porous medium,  $T_m$  is the mean fluid temperature,  $K_r$  is the thermal-diffusion ratio,  $Kr'$  is the chemical reaction constant and  $D$  is the mass diffusivity.

The radiative heat flux  $q_r'$  (under Rosseland approximation) has the form

$$q_r' = -\frac{4\sigma' \partial T'^4}{3k' \partial y'} \tag{5}$$

where  $k'$  – the mean absorption coefficient and  $\sigma'$  – the Stefan – Boltzmann constant. It is assumed that the temperature differences within the flow are sufficiently small such that  $T'^4$  may be expressed as a linear function of the temperature. This is accomplished by expanding  $T'^4$  in a Taylor series about  $T'_\infty$  using Taylor series expansion and neglecting the higher order terms, we get

$$T'^4 \cong 4T_\infty'^3 T' - 3T_\infty'^4$$

This gives

$$q_r' = -\frac{16a'\sigma T_\infty'^3 \partial T'}{3k' \partial y'} \tag{6}$$

From equation (6), equation (2) makes a reduction to the following form

$$\rho c_p \frac{\partial T'}{\partial t'} = \kappa \frac{\partial^2 T'}{\partial y'^2} + \frac{16a'\sigma T_\infty'^3}{3k'} \frac{\partial^2 T'}{\partial y'^2} - Q_0 (T' - T'_\infty) \tag{7}$$

The non-dimensional quantities are

$$y = y' 3 \sqrt{\frac{A}{\nu^2}}, u = \frac{u'}{3\sqrt{\nu A}}, t = t' 3 \sqrt{\frac{A^2}{\nu}}, \theta = \frac{T' - T'_\infty}{\frac{q_w''}{k} 3 \sqrt{\frac{\nu^2}{A}}}, C' = \frac{C' - C'_\infty}{C'_w - C'_\infty} \tag{8}$$

where  $f(t') = At'$ ,  $A$  – denotes the uniform acceleration of the plate in  $x$ -direction,  $u$  – dimensionless velocity,  $y$  – dimensionless coordinate perpendicular to the plate,  $\theta$  – dimensionless temperature,  $t$  – dimensionless time and  $\phi$  – dimensionless concentration.

Substituting equation (8) into the equations (1), (3) and (7) reduces in dimensionless form

$$\frac{\partial u}{\partial t} = \frac{\partial^2 u}{\partial y^2} - H Gr \theta + Gm \phi \tag{9}$$

$$F' \frac{\partial \theta}{\partial t} = \frac{1}{Pr} \frac{\partial^2 \theta}{\partial y^2} - L \theta \tag{10}$$

$$\frac{\partial \phi}{\partial t} = \frac{1}{Sc} \frac{\partial^2 \phi}{\partial y^2} - Kr \phi \tag{11}$$

The dimensionless initial and boundary conditions are

$$\begin{aligned} t \leq 0: \quad & u = 0, \quad \theta = 0, \quad \phi = 0 \quad \text{for all } y \geq 0 \\ t > 0: \quad & u = t, \quad \frac{\partial \theta}{\partial y} = -1, \quad \phi = 1 \quad \text{at } y = 0 \\ & u \rightarrow 0, \quad \theta \rightarrow 0, \quad \phi \rightarrow 0 \quad \text{as } y \rightarrow \infty \end{aligned} \tag{12}$$

where

$$\begin{aligned} M &= \frac{\sigma B_0^2 3\sqrt{v}A}{\rho A}, \quad Gr = \frac{\beta g q_w'' \sqrt{v}A}{\rho A}, \quad Gm = \frac{\beta' g (C'_\infty - C''_\infty)}{A} \\ \frac{1}{K} &= \frac{v\sqrt{v}A}{AK'}, \quad H = M + \frac{1}{K}, \quad Pr = \frac{v\rho c_p}{k}, \quad R = \frac{16a'T_\infty'^3}{3kk'}, \quad L = F'Q \\ Q &= \frac{Q_0}{\rho c_p 3\sqrt{\frac{A^2}{v}}}, \quad F' = \frac{Pr}{1+R}, \quad Sc = \frac{v}{D}, \quad Kr = Kr' \sqrt{\frac{v}{A^2}} \end{aligned} \tag{13}$$

where  $M$  – the magnetic field,  $Gr$  – thermal Grashof number,  $Pr$  is Prandtl number,  $Gc$  – modified Grashof number,  $Sc$  – Schmidt number,  $Kr$  – chemical reaction,  $K$  – porous permeability,  $Q$  – heat source parameter respectively.

### III. SOLUTION OF THE PROBLEM

Arranged for pictorial purpose of the problem defined by equations (9) – (11) solved by using perturbation technique. Exact analytical expression for dimensionless velocity field, temperature field and concentration field were separately obtained for  $Sc \neq 1, Sc = 1$ . Therefore the fluid in the neighbourhood of the fluid in the neighbourhood of the plate as

$$\begin{aligned} u &= u_0(y) + \varepsilon e^{at} u_1(y) + \dots \\ \theta &= \theta_0(y) + \varepsilon e^{at} \theta_1(y) + \dots \\ \phi &= \phi_0(y) + \varepsilon e^{at} \phi_1(y) + \dots \end{aligned} \tag{14}$$

Substituting (14) in equation (9) – (11) and equating the harmonic and non – harmonic terms, we obtain

$$u_0'' - Hu_0 = -Gr\theta_0 - Gm\phi_0 \tag{15}$$

$$u_1'' - \beta_3 u_1 = -Gr\theta_1 - Gm\phi_1 \tag{16}$$

$$\theta_0'' - L\theta_0 = 0 \tag{17}$$

$$\theta_1'' - \beta_1 \theta_1 = 0 \tag{18}$$

$$\phi_0'' - KrSc\phi_0 = 0 \tag{19}$$

$$\phi_1'' - \beta_2 \phi_1 = 0 \tag{20}$$

The corresponding boundary conditions are

$$\begin{aligned}
 u = 0, \theta = 0, \phi = 0 & \quad \text{for all } y \geq 0, t \leq 0 \\
 u_0 = t, u = 0, \frac{\partial \theta_0}{\partial y} = -1, \frac{\partial \theta_1}{\partial y} = 0 \quad \phi_0 = 1, \phi_1 = 0 & \quad \text{at } y = 0, t > 0 \\
 u_0 \rightarrow 0, \theta_0 \rightarrow 0, \phi_0 \rightarrow 0, u_1 \rightarrow 0, \theta_1 \rightarrow 0, \phi_1 \rightarrow 0 & \quad \text{as } y \rightarrow \infty
 \end{aligned}
 \tag{21}$$

**Case (i): For  $Sc \neq 1$**

Solving equations (15) – (20) under the boundary condition (21) and we obtain the velocity profiles, temperature profiles and concentration profiles in the boundary layer as

$$u_0 = L_1 e^{-\sqrt{L}y} + L_2 e^{-\sqrt{KrSc}y} + L_3 e^{-\sqrt{H}y}; u_1 = 0$$

$$\theta_0 = \frac{1}{\sqrt{L}} e^{-\sqrt{L}y}; \theta_1 = 0$$

$$\phi_0 = e^{-\sqrt{KrSc}y}; \phi_1 = 0$$

In view of the equation (14) becomes

$$u = L_1 e^{-\sqrt{L}y} + L_2 e^{-\sqrt{KrSc}y} + L_3 e^{-\sqrt{H}y}$$

$$\theta = \frac{1}{\sqrt{L}} e^{-\sqrt{L}y}$$

$$\phi = e^{-\sqrt{KrSc}y}$$

**Coefficient of Skin-Friction**

The coefficient of skin-friction at the vertical porous surface is given by

$$C_f = \left( \frac{\partial u}{\partial y} \right)_{y=0} = -\sqrt{L} L_1 - \sqrt{KrSc} L_2 - \sqrt{H} L_3$$

**Coefficient of Heat Transfer**

The rate of heat transfer in terms of Nusselt number at the vertical porous surface is given by

$$N_u = \left( \frac{\partial \theta}{\partial y} \right)_{y=0} = -1$$

**Sherwood number**

$$Sh = \left( \frac{\partial \phi}{\partial y} \right)_{y=0} = -\sqrt{KrSc}$$

**Case (ii): For  $Sc = 1$**

Solving Equations (15) – (20) under the boundary condition (21) and we obtain the velocity profiles, temperature profiles and concentration profiles in the boundary layer as

$$u_0 = L_1 e^{-\sqrt{L}y} + L_2 e^{-\sqrt{\gamma}y} + L_3 e^{-\sqrt{H}y}; u_1 = 0$$

$$\theta_0 = \frac{1}{\sqrt{L}} e^{-\sqrt{L}y}; \theta_1 = 0$$

$$\phi_0 = e^{-\sqrt{\gamma}y}; \phi_1 = 0$$

In view of the equation (14) becomes

$$u = L_1 e^{-\sqrt{L}y} + L_2 e^{-\sqrt{\gamma}y} + L_3 e^{-\sqrt{H}y}$$

$$\theta = \frac{1}{\sqrt{L}} e^{-\sqrt{L}y}$$

$$\phi = e^{-\sqrt{Kr}y}$$

### Coefficient of Skin-Friction

The coefficient of skin – friction at the vertical porous surface is given by

$$C_f = \left( \frac{\partial u}{\partial y} \right)_{y=0} = -\sqrt{L} L_1 - \sqrt{Kr} L_2 - \sqrt{H} L_3$$

### Coefficient of Heat Transfer

The rate of heat transfer in terms of Nusselt number at the vertical porous surface is given by

$$N_u = \left( \frac{\partial \theta}{\partial y} \right)_{y=0} = -1$$

### Sherwood number

$$Sh = \left( \frac{\partial \phi}{\partial y} \right)_{y=0} = -\sqrt{Kr}$$

## IV. RESULTS AND DISCUSSION

Final results are made for a noticeable of physical parameters, which are exhibited by means of graphs and the results are come into passion to give the effects of magnetic field parameter ( $M$ ), dimensionless permeability parameter ( $K$ ), Grashof numbers for heat and mass transfer ( $Gr, Gc$ ), chemical reaction parameter ( $Kr$ ), Prandtl number ( $Pr$ ), heat source parameter ( $Q$ ), radiation parameter ( $R$ ), Schmidt number ( $Sc$ ) and dimension less time ( $t$ ) on the velocity profiles, temperature profiles, concentration profiles, as well as the skin friction coefficient and Sherwood number. The velocity curves show that the rate of transport is remarkably reduced with increase for different values of magnetic parameter ( $M$ ) depicted in figure (2). These results were occurred qualitative manner with the expectations, since the magnetic field exerts a retarding effect on the natural convection flows. The variation of velocity profiles with dimensionless permeability parameter ( $K$ ) is shown in figure (3). From this figure clearly indicates that the value of velocity profiles increases with increasing the dimensionless permeability parameter. Physically, this result can be achieved when the holes of the porous medium are very large so that the resistance of the medium maybe neglected. Figure (4) is plotted to show the effect of thermal Grashof number ( $Gr$ ) on the velocity profiles. It is found that an increase in Grashof number lead to increase in the velocity. This is due to fact that buoyancy force enhances fluid velocity and increases the boundary layer thickness with increase in the values of Grashof number. It is also observed that distinctive peaks in the velocity profiles occur in the fluid adjacent to the wall for higher values of Grashof number. An invisible spiritual being felt to be nearby the peaks indicates that the maximum value of fluid velocity occurs in the body of the fluid close to the plate and not at the plate. Figure (5) depicts the effect of mass Grashof number ( $Gc$ ) on the velocity profiles, from this figure observed that, the effect of mass Grashof number on the fluid velocity is the same as that thermal Grashof number ( $Gr$ ). This statement is achieved by comparing figure (4) and (5). The velocity profiles lead to fall in the fluid for different values of chemical reaction parameter ( $Kr$ ) were observed in figure (6).



Figure (7) is sketched to show the effects of Prandtl number ( $Pr$ ) on velocity profiles. Four different realistic values of Prandtl number (0.71, 1.0, 7.0, 100) that are physically correspond to air, electrolytic solution, water and engine oil respectively are chosen. It is observed that the velocity decreases with increasing values of Prandtl number. This is due to the fact that fluid with large Prandtl number has high viscosity and small thermal conductivity, which make the fluid thick and causes a decrease in fluid velocity. The apparent effort of presence of the heat source parameter ( $Q$ ) on the velocity profiles on the boundary layer is shown in figure (8). It is obvious that an increasing the values of heat source parameter yield a decrease in the velocity distribution of the fluid. This is expected since the presence of a heat sink in the boundary layer absorbs energy. Which in turn cause the temperature of the fluid to decrease. This reduces in temperature produces a decrease in the flow field due to the buoyancy effect which couples the flow and thermal field. It is found that the velocity increases with increasing values of radiation parameter ( $R$ ) are shown in figure (9). This result happens due to the fact that the large radiation parameter values correspond to an increased dominance of conduction over radiation thereby increasing buoyancy force (thus, vertical velocity) and thickness of momentum boundary layer.

Figure (10) shows the effect of Schmidt number on the velocity profiles for  $Sc = 0.16$   $Sc = 0.3$   $Sc = 0.6$   $Sc = 2.01$  (i.e. hydrogen, helium, water vapour, ethyl Benzene). It is observed that the velocity decreases with increasing Schmidt number values due to the decrease in the molecular diffusivity, which results in a decrease in the concentration and velocity boundary layer thickness. Variation of velocity profiles for different values of dimensionless time ( $t$ ) is shown in figure (11). It is noticed that the velocity increases with the progression of time. Moreover, the velocity in this figure takes the values of time at the plate ( $y = 0$ ) and tends to zero for large values of  $y$ , which is a clear verification of the boundary conditions on the velocity given in equation (12).

Figure (12) has been plotted to depict the variation of temperature profiles against  $y$  for different values of heat source parameter ( $Q$ ) by fixing other parameters. It is observed from this graph that temperature decrease with increasing heat source parameter. It is observed in figure (13) that the temperature ( $\theta$ ) increases as the radiation parameter ( $R$ ) increases. This is because the large radiation parameter values correspond to an increased dominance of conduction over radiation thereby increasing the thickness of the thermal boundary layer. It is evident from figure (14), that as the values of Prandtl number ( $Pr$ ) increase we can find a decrease in the temperature profiles and hence there is a decrease in thermal boundary layer thickness and more uniform temperature distribution across the boundary layer. Physically, this behaviour is due to the fact that with increasing Prandtl number, the thermal conductivity of the fluid decreases and the fluid viscosity increases which in turn results in a decrease in the thermal boundary layer thickness. Figure (15) observes the influence of Schmidt number ( $Sc$ ) on the concentration ( $\phi$ ). It is evident from this figure that the increasing values of Schmidt number lead to fall in the concentration profiles. Physically, the increase of Schmidt number means a decrease of molecular diffusion  $D$ . Hence, the concentration of the species is higher for small values of Schmidt number and lower for large values of Schmidt number. The effect of chemical reaction parameter ( $Kr$ ) on the concentration ( $\phi$ ) is shown in figure (16). It is noticed from this figure that there is a marked effect of increasing values of on concentration distribution in the boundary layer. It is clearly observed from this figure that increasing values of decrease the concentration of species in the boundary layer.



This happens because large values of chemical reaction parameter reduce the solutal boundary layer thickness and increase the mass transfer. Figure (17) shows the variation of  $(\tau)$  versus magnetic field parameter  $(M)$  for different values of heat source parameter  $(Q)$  and dimensionless permeability parameter  $(K)$ . It is clear from this figure that for all values of magnetic parameter is decreased with an increase of  $K$  for all values of  $(Q)$ . A quite opposite attitude is shown on  $(\tau)$  with increasing values of  $Q$  for given  $M$  and  $K$ . Furthermore, and for all values of  $Q$  is induced as  $M$  increases during  $K = 0.5$ . As increase to 1, and when  $Q > 0.1$  is slightly decreased when  $M \leq M_0 \approx 0.4$  whereas the reverse effect is noticed when  $M > M_0$ . Moreover, the maximum effect of  $Q$  on  $\tau$  is attained in the hydrodynamic flow case  $(M = 0)$ , when the magnetic field is absent. It can be seen from figure (18) that the Sherwood number  $(Sh)$  is reduced with an increase of for all values of Schmidt number  $(Sc)$ . Also, this figure illustrates that with increasing values of  $Sc, Sh$  increasing when  $Kr \leq K_0 \approx 0.1$  and it is decreasing when  $Kr > K_0$ .

### Appendix

$$\beta_1 = (1 + F^*at), \beta_2 = (Kr + at)Sc, \beta_3 = (H + at)$$

$$L_1 = -\frac{Gr}{\sqrt{L}(L-H)}, L_2 = -\frac{Gm}{KrSc-H}, L_3 = (t - L_1 - L_2)$$

### REFERENCES

- [1] A J Chamkha (2000): *Thermal radiation and buoyancy effects on hydromagnetic flow over an accelerating permeable surface with heat source or sink*. *International Journal of Engineering Science*, 38 (15), pp. 1699-1712.
- [2] A J Chamkha (2004): *Unsteady MHD convective heat and mass transfer past a semi infinite vertical permeable moving plate with heat absorption*. *International Journal of Engineering Science*, 42 (2), pp. 217-230.
- [3] A N Donald and A Bejan (2006): *Convection in porous media*, Springer Science & Business Media.
- [4] D Ch Kesavaiah, P V Satyanarayana and S Venkataramana (2011): *Effects of the chemical reaction and radiation absorption on an unsteady MHD convective heat and mass transfer flow past a semi-infinite vertical permeable moving plate embedded in a porous medium with heat source and suction*, *Int. J. of Appl. Math and Mech. Vol. 7 (1)*, pp. 52-69.
- [5] D Ch Kesavaiah, P V Satyanarayana, J Gireesh Kumar and S Venkataramana (2012): *Radiation and mass transfer effects on moving vertical plate with variable temperature and viscous Dissipation*, *International Journal of Mathematical Archive*, Vol. 3 (8), pp. 3028-3035
- [6] Damala Ch Kesavaiah, P V Satyanarayana and S Venkataramana (2012): *Radiation absorption, chemical reaction and magnetic field effects on the free convection and mass transfer flow through porous medium with constant suction and constant heat flux*, *International Journal of Scientific Engineering and Technology*, Vol.1 (6), pp. 274-284
- [7] M A Sattar (1994): *Free convection and mass transfer flow through a porous medium past an infinite vertical porous plate with time dependent temperature and concentration*. *Ind. J. Pure Appl. Math*, 23, pp.759-766.
- [8] M A Seddeek, A A Darwish and M S Abdelmeguid (2007): *Effects of chemical reaction and variable viscosity on hydromagnetic mixed convection heat and mass transfer for biemenz flow through porous media with radiation*. *Communications in Nonlinear Science and Numerical Simulation*, Vol. 12 (2), 195-213.
- [9] M M Rahman and M A Sattar (2006): *Magnetohydrodynamic convective flow of a micropolar fluid past a continuously moving vertical porous plate in the presence of heat generation/absorption*, *Journal of Heat Transfer*, 128 (2), pp. 142-152.

- [10] *Mohamed Abd El-aziz, Aishah Syahya (2017): Heat and mass transfer of unsteady hydromagnetic free convection flow through porous medium past a vertical plate with uniform surface heat flux, Journal of theoretical and applied mechanics, Sofia, vol. 47 no. 3, pp. 25-58*
- [11] *T Hayat and Z Abbas (2008): Heat transfer analysis on the MHD flow of a second grade fluid in a channel with porous medium. Chaos, Solitons & Fractals, 38 (2), pp. 556-567.*
- [12] *Damala Ch Kesavaiah, P V Satyanarayana and A Sudhakaraiah: Effects of radiation and free convection currents on unsteady Couette flow between two vertical parallel plates with constant heat flux and heat source through porous medium, International Journal of Engineering Research, 2013, Vol. 2 (2), pp. 113-118, ISSN : 2319-6890*
- [13] *S Karunakar Reddy, D Chenna Kesavaiah and M N Raja Shekar (2013): MHD heat and mass transfer flow of a viscoelastic fluid past an impulsively started infinite vertical plate with chemical reaction, International Journal of Innovative Research in Science, Engineering and Technology, Vol. 2 (4), pp.973- 981, ISSN: 2319-8753*
- [14] *D Ch Kesavaiah, P V Satyanarayana, J Gireesh Kumar and S Venkataramana (2012): Radiation and mass transfer effects on moving vertical plate with variable temperature and viscous Dissipation, International Journal of Mathematical Archive, Vol. 3 (8), pp. 3028-3035, ISSN: 2229-5046*
- [15] *D Chenna Kesavaiah, P V Satyanarayana and S Venkataramana (2013): Radiation and Thermo - Diffusion effects on mixed convective heat and mass transfer flow of a viscous dissipated fluid over a vertical surface in the presence of chemical reaction with heat source, International Journal of Scientific Engineering and Technology, Vol. 2 (2), pp: 56-72, ISSN : 2277-1581*
- [16] *Damala Ch Kesavaiah, P V Satyanarayana and S Venkataramana (2012): Radiation absorption, chemical reaction and magnetic field effects on the free convection and mass transfer flow through porous medium with constant suction and constant heat flux, International Journal of Scientific Engineering and Technology, pp. 274-284, Vol.1 (6), ISSN: 2277-1581*

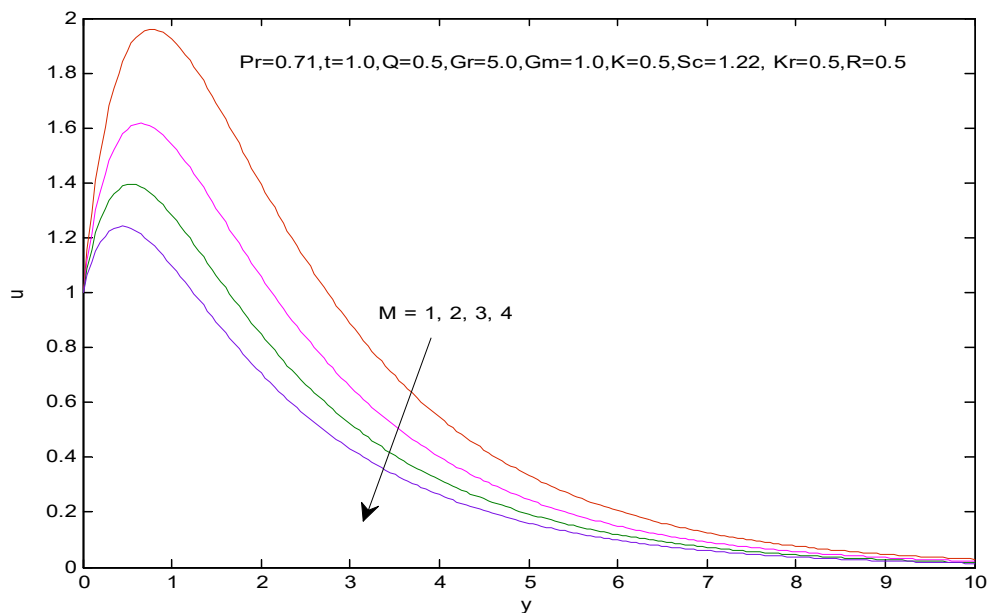


Figure (2): Velocity profiles for different values of M

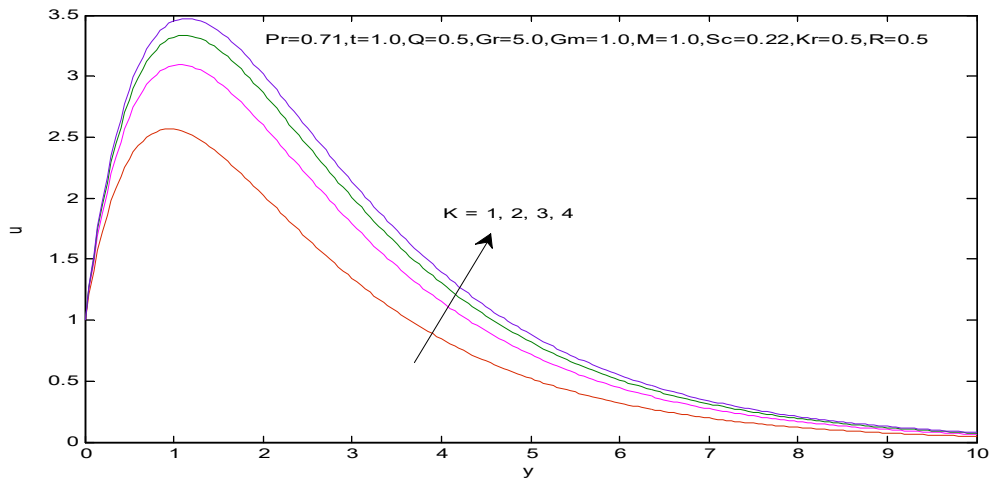


Figure (3): Velocity profiles for different values of  $K$

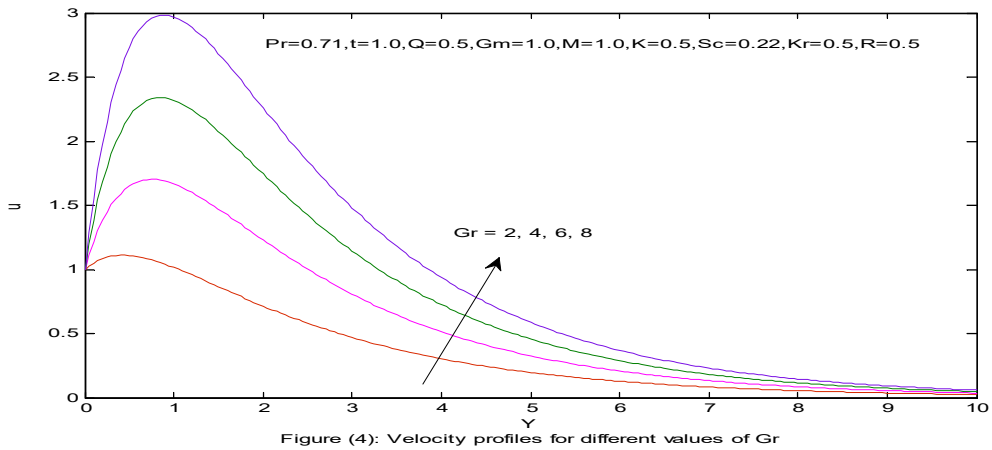


Figure (4): Velocity profiles for different values of  $Gr$

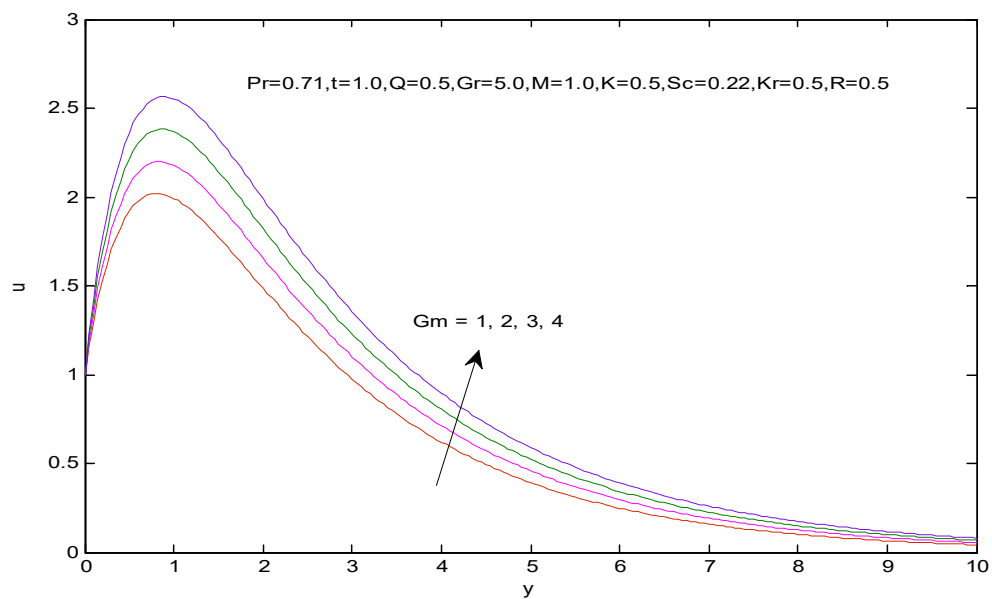


Figure (5): Velocity profiles for different values of  $Gm$

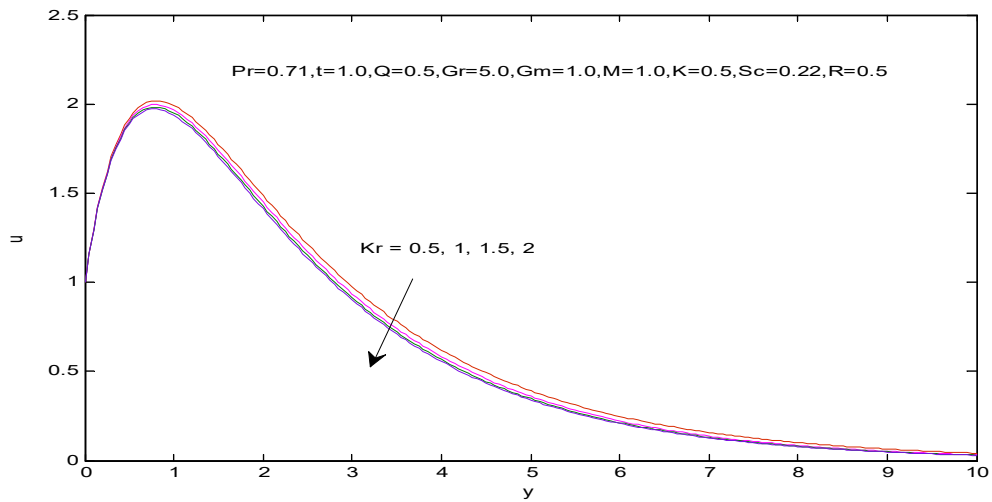


Figure (6): Velocity profiles for different values of Kr

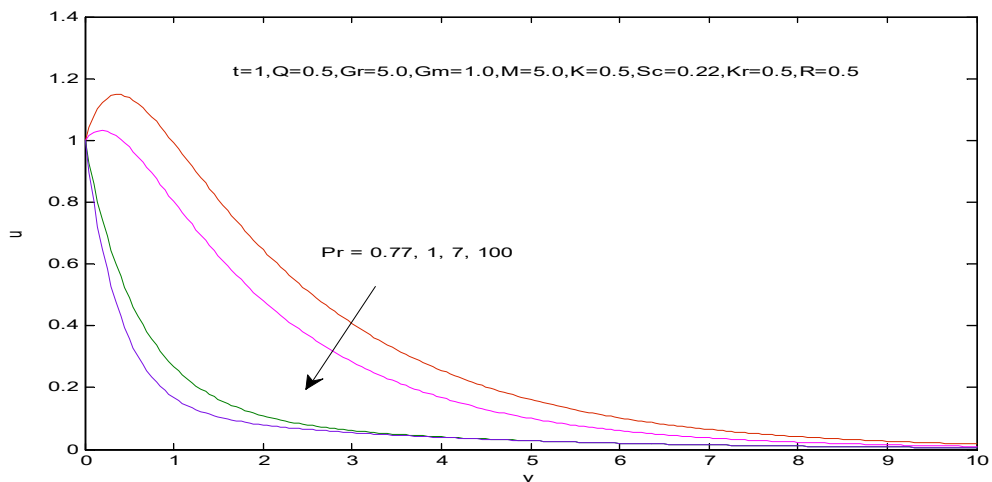


Figure (7): Velocity profiles for different values of Pr

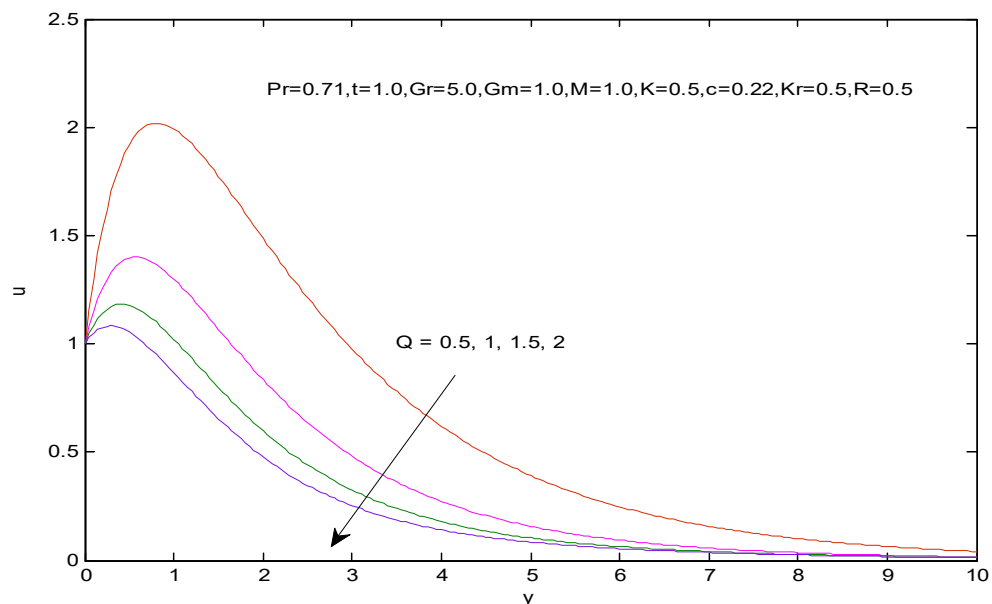


Figure (8): Velocity profiles for different values of Q

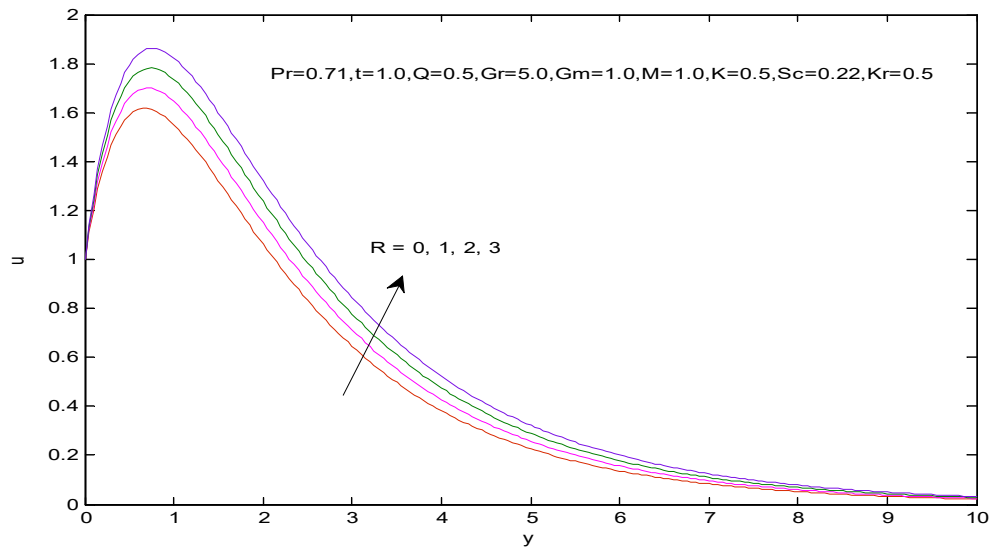


Figure (9): Velocity profiles for different values of  $R$

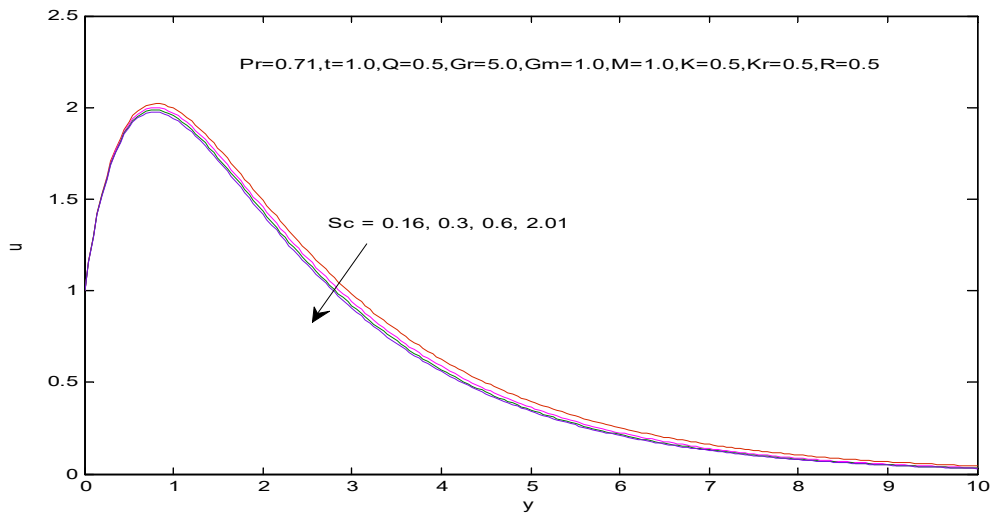


Figure (10): Velocity profiles for different values of  $Sc$

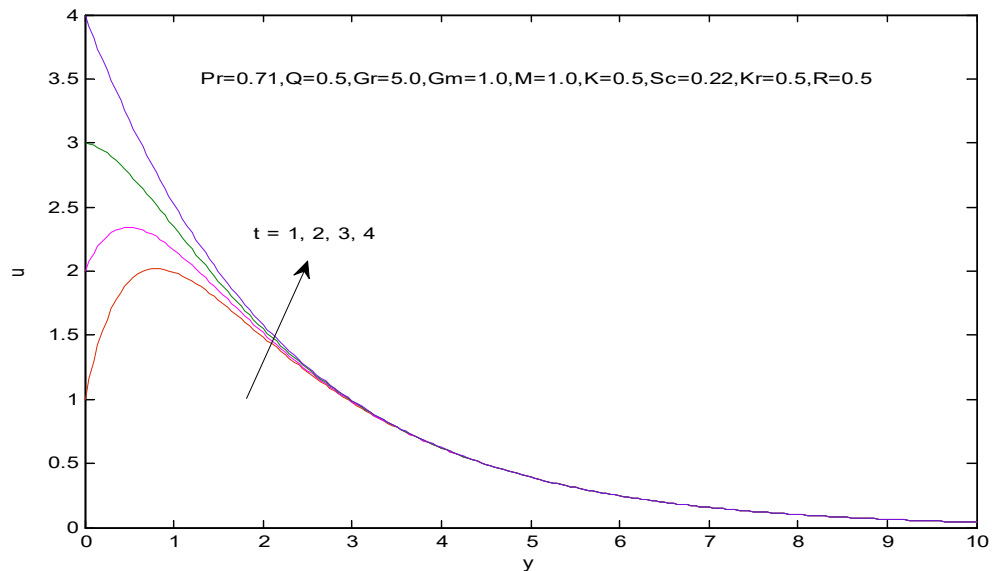


Figure (11): Velocity profiles for different values of  $t$

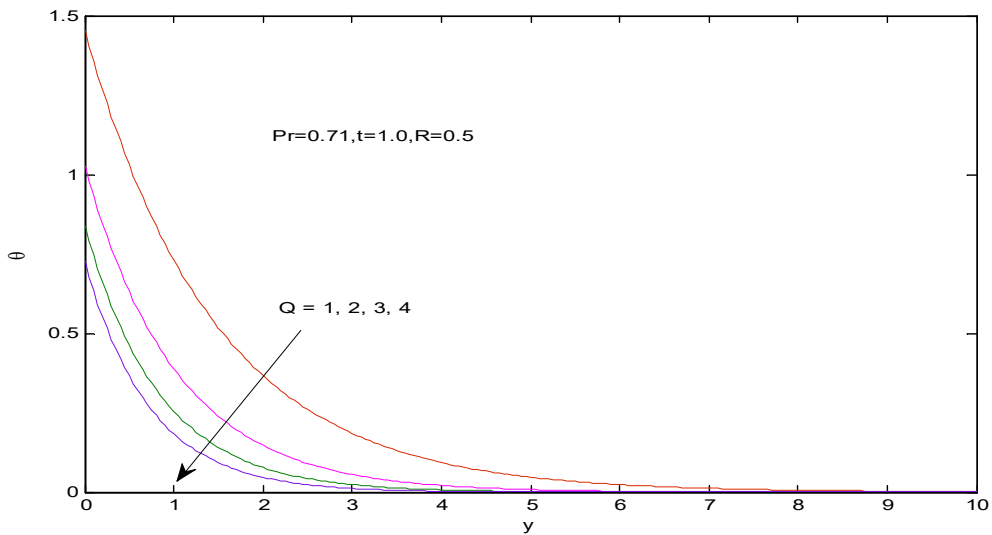


Figure (12): Temperature profiles for different values of  $Q$

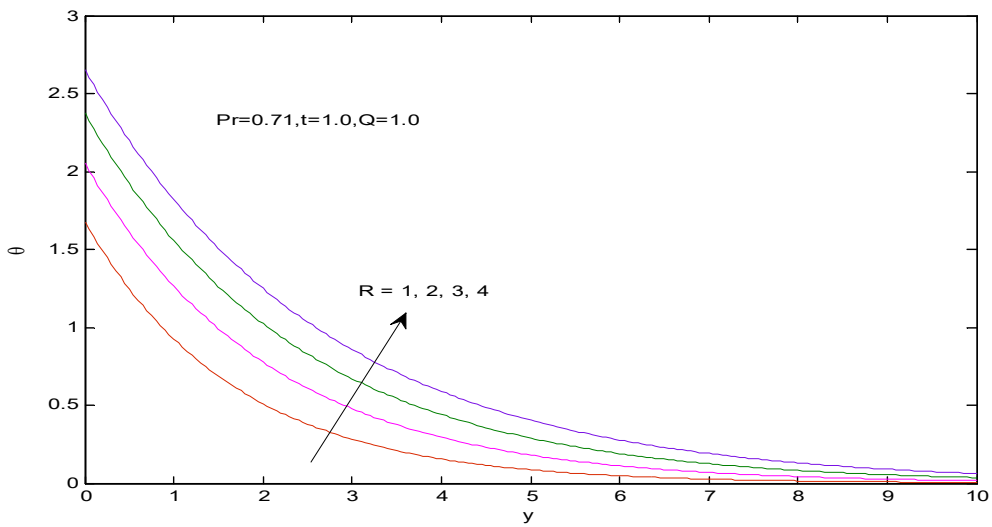


Figure (13): Temperature profiles for different values of  $R$

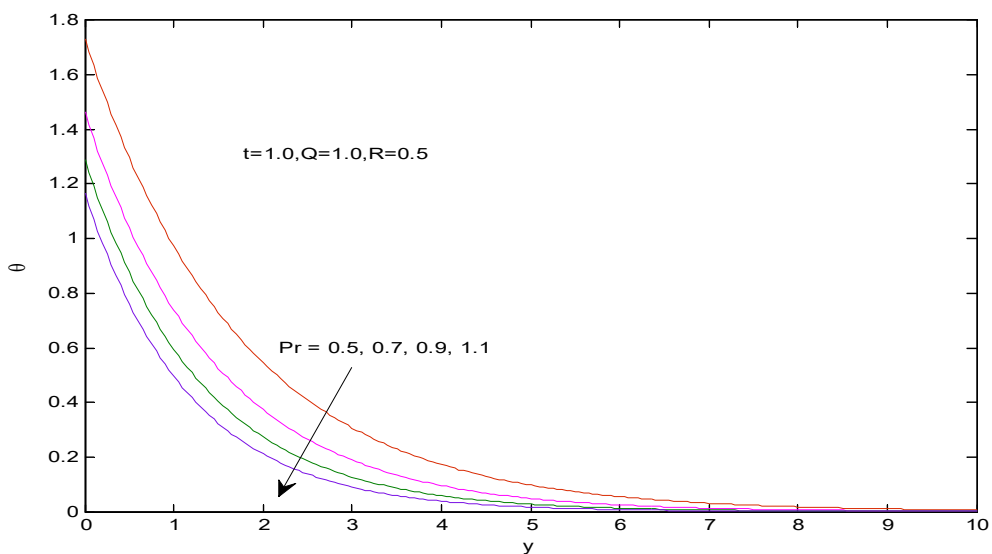


Figure (14): Temperature profiles for different values of  $Pr$

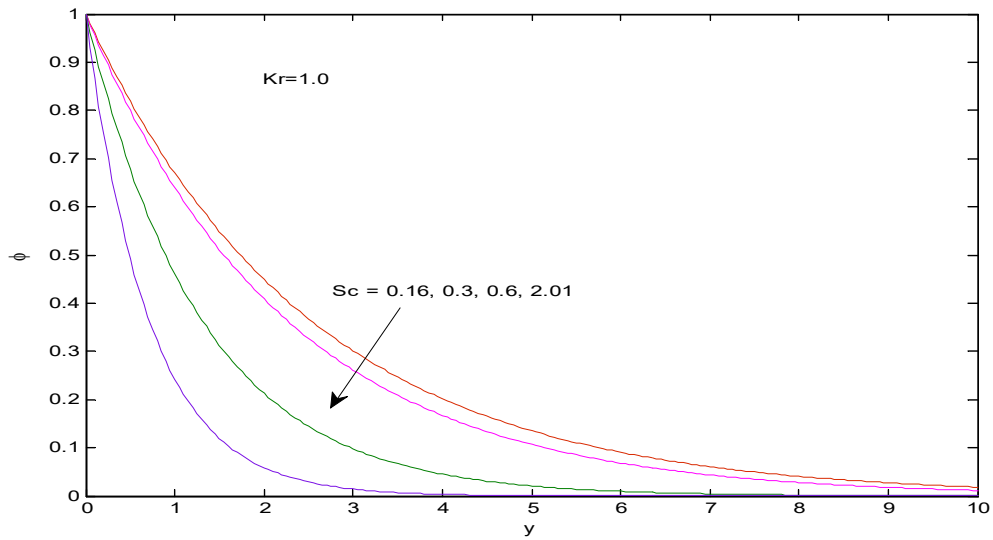


Figure (15): Concentration profiles for different values of Sc

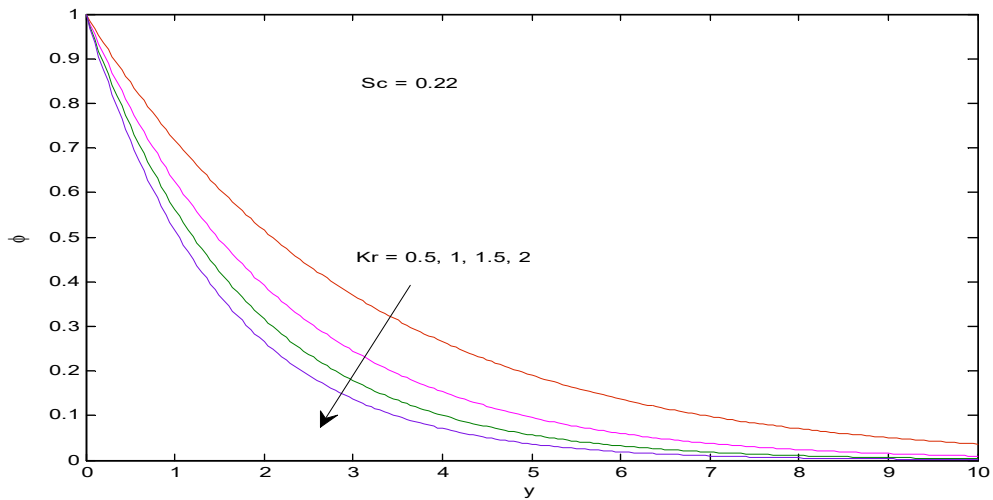


Figure (16): Concentration profiles for different values of Kr

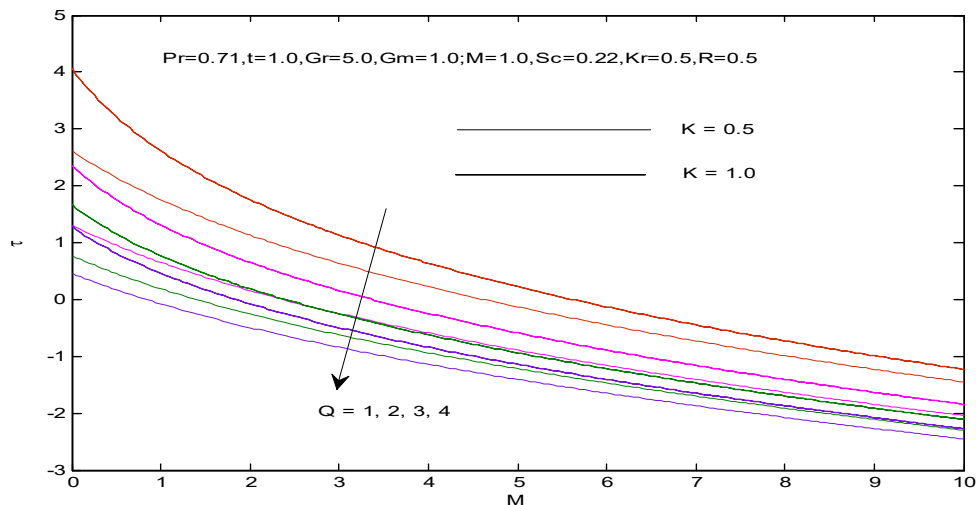


Figure (17): Skin friction variation for various values of Q



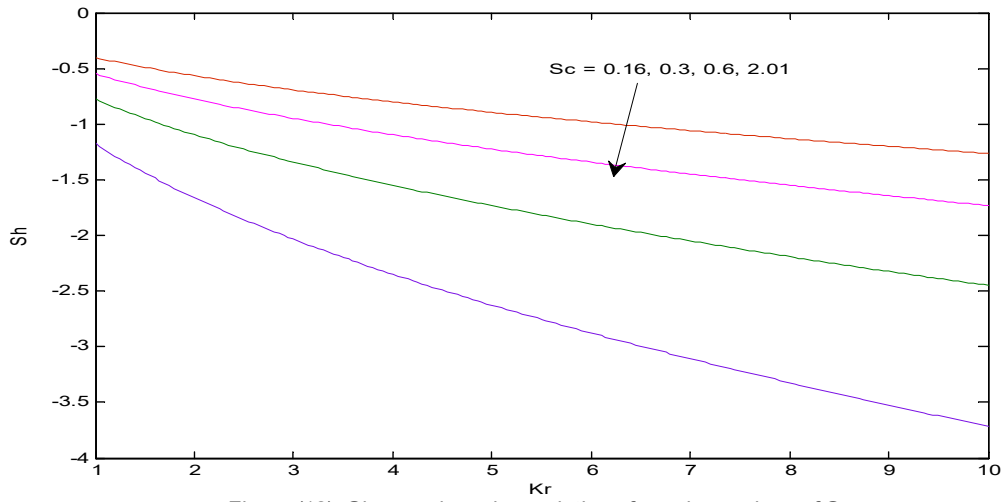


Figure (18): Sherwood number variations for various values of Sc